Monthly Notices
of the
ROYAL ASTRONOMICAL SOCIETY

MNRAS **476,** L15–L19 (2018)
Advance Access publication 2018 February 10

doi:10.1093/mnrasl/sly023

Direct Lyman continuum and Ly α escape observed at redshift 4

E. Vanzella,[1⋆] M. Nonino,[2⋆] G. Cupani,[2] M. Castellano,[3] E. Sani,[4] M. Mignoli,[1] F. Calura,[1] M. Meneghetti,[1] R. Gilli,[1] A. Comastri,[1] A. Mercurio,[5] G. B. Caminha,[6] K. Caputi,[6] P. Rosati,[1,7] C. Grillo,[8,9] S. Cristiani,[2] I. Balestra,[10] A. Fontana[3] and M. Giavalisco[11]

[1]*INAF – Osservatorio Astronomico di Bologna, via Gobetti 93/3, I-40129, Bologna, Italy*
[2]*INAF – Osservatorio Astronomico di Trieste, via G. B. Tiepolo 11, I-34143, Trieste, Italy*
[3]*INAF – Osservatorio Astronomico di Roma, Via Frascati 33, I-00078, Monte Porzio Catone (RM), Italy*
[4]*European Southern Observatory, Alonso de Cordova 3107, Casilla 19, Santiago 19001, Chile*
[5]*INAF – Osservatorio Astronomico di Capodimonte, Via Moiariello 16, I-80131, Napoli, Italy*
[6]*Kapteyn Astronomical Institute, University of Groningen, Postbus 800, NL-9700, AV Groningen, The Netherlands*
[7]*Dipartimento di Fisica e Scienze della Terra, Università degli Studi di Ferrara, via Saragat 1, I-44122, Ferrara, Italy*
[8]*Dipartimento di Fisica, Università degli Studi di Milano, via Celoria 16, I-20133 Milano, Italy*
[9]*Dark Cosmology Centre, Niels Bohr Institute, University of Copenhagen, Juliane Maries Vej 30, DK-2100 Copenhagen, Denmark*
[10]*University Observatory Munich, Scheinerstrasse 1, D-81679 Munich, Germany*
[11]*Astronomy Department, University of Massachusetts, Amherst, MA 01003, USA*

Accepted 2018 February 6. Received 2018 January 25; in original form 2017 December 19

ABSTRACT

We report on the serendipitous discovery of a $z = 4.0$, $M_{1500} = -22.20$ star-forming galaxy (*Ion3*) showing copious Lyman continuum (LyC) leakage (∼60 per cent escaping), a remarkable multiple peaked Ly α emission, and significant Ly α radiation directly emerging at the resonance frequency. This is the highest redshift confirmed LyC emitter in which the ionizing and Ly α radiation possibly share a common ionized channel (with $N_{\rm H\,I} < 10^{17.2}$ cm^{-2}). *Ion3* is spatially resolved, it shows clear stellar winds signatures like the P-Cygni N vλ1240 profile, and has blue ultraviolet continuum ($\beta = -2.5 \pm 0.25$, $F_\lambda \sim \lambda^\beta$) with weak low-ionization interstellar metal lines. Deep VLT/HAWKI Ks and Spitzer/IRAC 3.6 and 4.5μm imaging show a clear photometric signature of the H α line with equivalent width of 1000 Å rest-frame emerging over a flat continuum (Ks−4.5μm $\simeq$ 0). From the SED fitting, we derive a stellar mass of 1.5×10^9 M$_\odot$, SFR of 140 M$_\odot$ yr^{-1} and age of ∼10 Myr, with a low dust extinction, $E(B-V) \lesssim 0.1$, placing the source in the starburst region of the SFR−M* plane. *Ion3* shows similar properties of another LyC emitter previously discovered ($z = 3.21$, *Ion2*, Vanzella et al. 2016). *Ion3* (and *Ion2*) represents ideal high-redshift reference cases to guide the search for reionizing sources at $z > 6.5$ with JWST.

Key words: gravitational lensing: strong – galaxies: formation – galaxies: starburst – ultraviolet: general.

1 INTRODUCTION

The definition of a reference sample of Lyman continuum (LyC) emitters at $z \lesssim 4.5$ is crucial to guide the identification of the sources that reionized the Universe at $z > 6.5$, an epoch when the LyC is not directly observable (Worseck et al. 2014). Several LyC leakers showing escape fraction of $f_{esc}^{abs} \sim 4-15$ per cent have been confirmed in the nearby universe, $z \sim 0$–0.3 (see Izotov et al. 2016a,b and references therein). Recently, Izotov et al. (2017) identified another LyC emitter with $f_{\rm esc} \simeq 46$ per cent, the highest value currently measured for the local sample. Most searches at high redshift have proved unsuccessful, due to contamination by foreground sources (Siana et al. 2015), or have yielded fairly stringent limits of $f_{\rm esc} < 0.1$ (e.g. Vanzella et al. 2012; Grazian et al. 2017). However, three LyC emitters have been confirmed at cosmological distances, $2.5 < z < 3.2$ with $f_{\rm esc} \sim 30-100$ per cent (de Barros et al. 2016; Shapley et al. 2016; Vanzella et al. 2016; Bian et al. 2017). As shown in Verhamme et al. (2017) the available sample of LyC leakers, both at low and high redshift, show very consistent observational features. Such features include the high Ly α equivalent width EW >40Å, a high ratio of [O III]λ5007/ [O II]λ3727, and narrow signatures in the Ly α emission like narrow double peaked profiles (<300–400 km s^{-1}) or Ly α emission close to the

⋆ E-mail: vanzella@oabo.inaf.it (EV); nonino@oats.inaf.it (MN)

systemic velocity ($<100\,\mathrm{km\,s^{-1}}$). Also intense nebular optical lines [O III]λλ4959, 5007+ H β with EW of 1000–1500 Årest-frame seem often associated with LyC emitters (e.g. Schaerer et al. 2016), as well as their compact star-forming region (Heckman et al. 2011) and the weakness of the low-ionization interstellar absorption lines (e.g. Jones et al. 2013; Chisholm et al. 2017). Overall, these quantities correlate with $f_{\rm esc}$, as was predicted by radiation transfer models (Verhamme et al. 2015) and photoionization models (e.g. Jaskot & Oey 2013; Zackrisson, Inoue & Jensen 2013; Nakajima & Ouchi 2014). In this work, we report on a serendipitously discovered LyC emitter at redshift 4, dubbed here *Ion3*, the highest redshift case currently known. We assume a flat cosmology with $\Omega_{\rm M} = 0.3$, $\Omega_{\Lambda} = 0.7$, and $H_0 = 70\,\mathrm{km\,s^{-1}\,Mpc^{-1}}$.

2 DATA: FORS AND X-SHOOTER OBSERVATIONS

Ion3 was discovered during a FORS2 spectroscopic program executed in visitor mode during the period 2017 September 15–19 (prog. 098.A-0804(B), P.I. Vanzella). *Ion3* is a relatively bright object and was inserted as a filler in the MXU FORS mask (*I*-band magnitude 23.64 ± 0.38) and located at $3'41''$ from the Frontier Field galaxy cluster AS1063 (Lotz et al. 2017), which lies outside the HST coverage. Given the large separation from the galaxy cluster the resulting magnification is low, a well-constrained $\mu = 1.15 \pm 0.02$ (or $\Delta m = 0.15$, Caminha et al. 2016). In the following, all the reported quantities are corrected for μ.

The data reduction was carried on as described in several previous works (e.g. Vanzella et al. 2014) in which the AB-BA sky subtraction scheme was implemented. The final spectrum consists of 14 h integration with an average seeing of 0.8 arcsec and spectral resolution $\mathrm{d}v \simeq 600\ \mathrm{km\,s^{-1}}$ at $\lambda = 7000$ Å ($R = \lambda/\mathrm{d}\lambda = 500$, grism 300V). Fig. 1 shows the FORS2 spectrum covering the wavelength range 3700–9300Å. During the same program 098.A-0804(B), an additional 1 h integration was obtained with the grism 600B, doubling the spectral resolution ($\mathrm{d}v \simeq 300\ \mathrm{km\,s^{-1}}$, $R = 1000$). We clearly confirmed the double peaked Ly α profile of *Ion3* not well resolved with the 300V grating (see Fig. 1, top left). Additional four hours X-Shooter integration on *Ion3* was subsequently obtained during 2017 November with an average seeing conditions of 0.8 arcsec (prog. 098.A-0665, P.I. Vanzella), providing a final spectrum spanning the range 3 400–24 000 Å with spectral resolution $\mathrm{d}v \simeq 35 - 60\,\mathrm{km\,s^{-1}}$. We refer the reader to Vanzella et al. (2014, 2017) for details about FORS and X-Shooter data reduction.

3 RESULTS

3.1 The Lyman continuum emission

The most intriguing feature emerging from *Ion3* is the LyC leakage at $\lambda < 912$ Å rest-frame detected in the FORS spectrum with S/N=6.4(11.1) if averaged over the interval 880–910(800–910Å), and corresponding to magnitude 27.5 (AB). Fig. 1 shows the two-dimensional spectrum with the LyC signal spatially aligned with the non-ionizing radiation. The possible presence of a foreground object at $z < 4$ mimicking the LyC signal represents a serious problem in this kind of observations (e.g. Vanzella et al. 2012; Siana et al. 2015), especially when HST imaging is not available. However, we can reasonably exclude such an interloper. First, we note that the probability chance of a superposition is low, less than 1 per cent adopting the above magnitude and the seeing of 0.8 arcsec (see Vanzella et al. 2010). Secondly, there is no trace of any spectral line

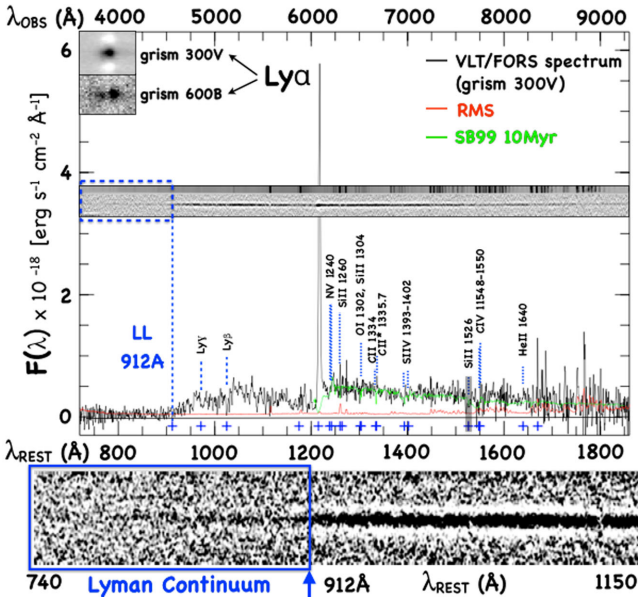

Figure 1. The FORS spectrum at resolution $\mathrm{d}v \simeq 580\ \mathrm{km\,s^{-1}}$ (grism 300V) of *Ion3* is shown along with the most relevant ultraviolet lines. In the top-left insets the Ly α spectra at resolution $\mathrm{d}v \simeq 300(580)\ \mathrm{km\,s^{-1}}$ obtained with the grism 600B(300V) are shown. The two-dimensional signal to noise and sky spectra are shown in the middle of the figure, in which the wavelength coverage up to 9300 Å is well sampled, despite the fringing pattern at $\lambda > 7800$ Å typical of the E2V blue-optimized CCD. In the bottom the the emerging LyC with S/N>10 is clearly detected.

arising from a foreground object, both in the deep FORS spectrum (that excludes [O II]λ3727, 3729 at $z < 1.45$ and Ly α at $z > 1.9$) and wide X-Shooter spectrum, that easily would have captured several UV and/or optical rest-frame emission lines in the redshift range $0 < z < 4$. Moreover, all the properties of *Ion3* support a very low column density of neutral gas along the line of sight, making the entire picture consistent with the emerging LyC signal.

From the FORS spectrum the observed fluxes at 900 and 1500 Årest-frame are $F_{\lambda}^{900} = (5.6 \pm 0.08) \times 10^{-20}\,\mathrm{erg\,s^{-1}\,cm^{-2}\,\AA^{-1}}$ and $F_{\lambda}^{1500} = (3.8 \pm 0.09) \times 10^{-19}\,\mathrm{erg\,s^{-1}\,cm^{-2}\ \AA^{-1}}$, respectively, corresponding to a flux density ratio of $f_{\nu}(1500)/f_{\nu}(900) = 19.1 \pm 3.3$. Following Vanzella et al. (2012), this ratio translates to a relative escape fraction *fesc,rel* = 20–100 per cent, assuming an intrinsic ratio of the luminosity densities $L_{\nu}(1500)/L_{\nu}(900) = 1$–5 and the median intergalactic medium (IGM) transmission at 900Å, $< T_{\rm IGM}^{900} >= 0.26$ (with a central 68 per cent interval of 0.05–0.40, Inoue et al. (2014); Vanzella et al. (2015). Being a single line of sight the real $T_{\rm IGM}^{900}$ is unknown, therefore, any combination of $L_{\nu}(1500)/L_{\nu}(900) > 1$ and IGM transmission lower than 100 per cent produces *fesc,rel* in the range 10 per cent–100 per cent, with a fiducial value of 60 per cent adopting median $< T_{\rm IGM}^{900} >= 0.26$ and $L_{\nu}(1500)/L_{\nu}(900) = 3$. The inferred ionizing photon production rate from F_{λ}^{900} is $N_{\rm phot}(900) = 3.5 \times 10^{53}\,\mathrm{s^{-1}}$, which compared to Starburst99 models for instantaneous bursts (Salpeter IMF; Salpeter 1955, and upper mass limit of 100 $\mathrm{M_{\odot}}$; Leitherer et al. 2014) yields a stellar mass involved in the starburst event of $4 \times 10^6\ \mathrm{M_{\odot}}$ with the age not larger than 20 Myrs, and a number of O-type stars dominating the ionizing radiation of $\simeq 1.6 \times 10^4$ (with uncertainties mainly dominated by the aforementioned IGM transmission).

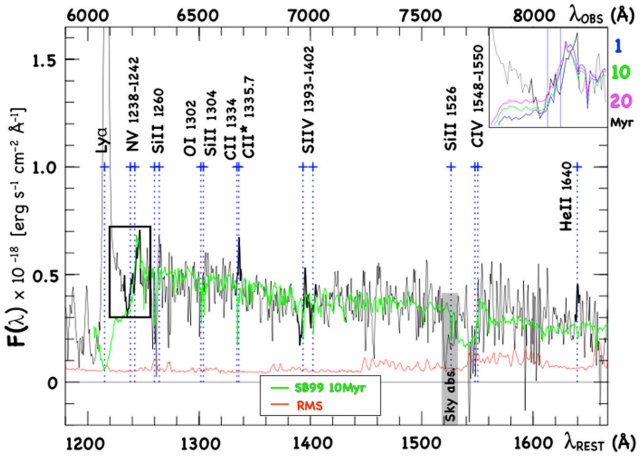

Figure 2. The FORS spectrum is shown with the main spectral features reported at the systemic redshift (blue crosses). In particular, the P-Cygni N vλ1240, [C II]*λ1335.71, [S IV]λ1393, 1402, and the He IIλ1640 lines are highlighted with thick lines. The N vλ1240 region (square) is zoomed and shown in the top-right inset (black line), in which three Starburst99 stellar models of 1, 10, and 20 Myr are superimposed to the spectrum (coloured lines).

3.2 The non-ionizing properties

The continuum redward the Ly α line up to $\simeq$ 1850 Å rest-frame is well detected in the FORS spectrum (Figs 1 and 2) with a best-fitting ultraviolet spectral slope of $\beta = -2.50$ with 68 per cent central interval $[-2.73,-2.28]$ ($F_\lambda \sim \lambda^\beta$).

Such a steep slope is not significantly affected by the atmospheric dispersion (the atmospheric dispersion compensator, LADC, is part of the system at UT1), and is fully consistent with being powered by massive and hot stars (O and early B stars), which are also responsible for the ionizing photons. The strongest spectroscopic signature of these stars is provided by the broad P-Cygni profiles in the resonance transitions of highly ionized species that arise in the stellar winds (e.g. Leitherer et al. 2014). In our FORS spectrum, a N vλ1240 P-Cygni profile is clearly present (see Fig. 2), observed also in local star-forming galaxies (e.g. Heckman et al. 2011, see also fig. 4 of Jaskot et al. 2017). In particular, the height and depth of the N vλ1240 line suggest an age of the burst of a few Myr. We superimposed a Starburst99 (Leitherer et al. 2014) spectral population synthesis model to the FORS spectrum with instantaneous burst with age 1, 10, and 20 Myr old, 0.4 solar metallicity (Salpeter IMF and 100 $M_\odot$ upper mass limit), which reproduces the observations well (especially the 1–10 Myr old templates, Fig. 2). Low ionization interstellar absorption lines like [Si II]λ1260, [O I]λ1303, and [C II]λ1334 are very weak or even absent, indicating a very low gas covering fraction consistent with the measured LyC leakage (Heckman et al. 2011; Jones et al. 2013; Chisholm et al. 2017). Interestingly, *Ion3* also shows the non-resonant fluorescent emission line [C II]*λ1335.71 (see Fig. 2). Such a feature has been detected by Jaskot & Oey (2014) on local LyC candidates and interpreted as an evidence of the complex geometry of the neutral gas outside the line of sight, like anisotropic ionizing emission. The systemic redshift z_{sys} has been derived from the [C II]*λ1335.71 line and more accurately from the X-Shooter detection of the [O II]λ3727, 3729 doublet, providing $z_{sys} = 3.999 \pm 0.001$. At such redshift, the doublet [N v]$\lambda\lambda$1239, 1243 lies in the middle of its P-Cygni profile and the possible He IIλ1640 line is also recognized, though with low significance, 2.7σ. Table 1 summarizes the most relevant spectroscopic properties.

Table 1. Spectral and physical properties of *Ion3*. Line fluxes are reported in units of 10^{-17} erg s^{-1} cm^{-2} (no slit losses are considered). Quantities are corrected for the lensing magnification $\mu = 1.15$. σ_z is the redshift error on the last digit.

Line/λ_{vacuum}	Flux(S/N)	z[σ_z], Resolution(km s^{-1})
Ly α(0) 1215.7	0.37(5)	3.9902[4], 35 (XSHO)
Ly α(1) 1215.7	1.16(12)	3.9950[3], 35 (XSHO)
Ly α(2) 1215.7	1.37(15)	3.9984[3], 35 (XSHO)
Ly α(3) 1215.7	6.23(32)	4.0033[3], 35 (XSHO)
Ly α(total)	9.13(73)	–, 580 (FORS)
[C II]*λ1335.71	0.14(4)	4.000[4], 580 (FORS)
[He II] λ1640.42	0.12(2.7)	4.000[4], 580 (FORS)
[O II] λ3727.09	0.38(4.5)	3.999[1], 55 (XSHO)
[O II] λ3729.88	0.25(3)	3.999[1], 55 (XSHO)
SED-fitting output	Value	Uncertainty
M(stellar) ($\times 10^9$ $M_\odot$)	1.5	[1.4–2.2]
Age (Myr)	11	[10–20]
SFR [$M_\odot$yr^{-1}]	140	[110–150]
$E(B-V)$	$\simeq$ 0.1	[0–0.1]
M_{UV}(1500)	−22.20	±0.15
H α EW(rest) (Å)	$\simeq$ 1000	[700–1300]
Nphot(900Å)(s^{-1})	3.0×10^{53}	[10^{53-54}]
$\log_{10}(\xi_{ion}$(Hz erg^{-1}))	25.6	25.4–25.8
$f_{esc,\,rel}$	0.60	[0.10–1.00]

3.3 The multiple peaked Ly α emission

In the conventional scenario for Ly α emission, Ly α scatters many times before escaping, which significantly alters and broadens the original line profile. The kinematics, the column density, and geometry of the H I gas are the main ingredients that shape the Ly α emission (not to mention the dust attenuation). A prominent Ly α emission line with rest-frame EW $= 40 \pm 3$ Å is clearly detected in the FORS spectrum (Fig. 1). Fig. 3 shows the same line at the X-Shooter spectral resolution (d$v = 35$ km s^{-1}), in which we identify four emitting structures marked as 0, 1, 2, and 3. While the presence of blue peaks typically suggest a low column of H I gas (e.g. Henry et al. 2015; Yang et al. 2016), the emission at peak (2) is remarkable and emerges at the resonance frequency ($z = 3.9984$, i.e. $\lesssim$ 40 km s^{-1} from the systemic), where the opacity to Ly α photons would be the highest (Fig. 3). This is fully consistent with a scenario in which the LyC and (part of) the Ly α photons are escaping along the same optically thin direction (to LyC, $N_{HI} < 10^{17.2}$ cm^{-2}) and likely from the same cavity (e.g. Zackrisson, Inoue & Jensen 2013; Behrens, Dijkstra & Niemeyer 2014; Verhamme et al. 2015). The LyC−Ly α escape through a ionized channel discussed in Behrens et al. (2014) consider the possibility that the gas is outflowing perpendicular to a galactic disc (and is reminiscent of a wind breaking out of a galactic disk). In this scenario, the quadruply peaked Ly α emission observed in *Ion3* might be associated with a face-on disc. *Ion3* represents the highest redshift empirical evidence of such a LyC−Ly α escaping mode. The Ly α escape degenerates with the H I column and the outflow velocity such that fast winds can mimic low columns (Verhamme et al. 2015). In this case, both the LyC emission and a relatively fast wind are detected. The evidence of an outflowing gas is imprinted in the blueshifted interstellar metal lines [S IV]λ1393.76 and [S IV]λ1402.77, with an average

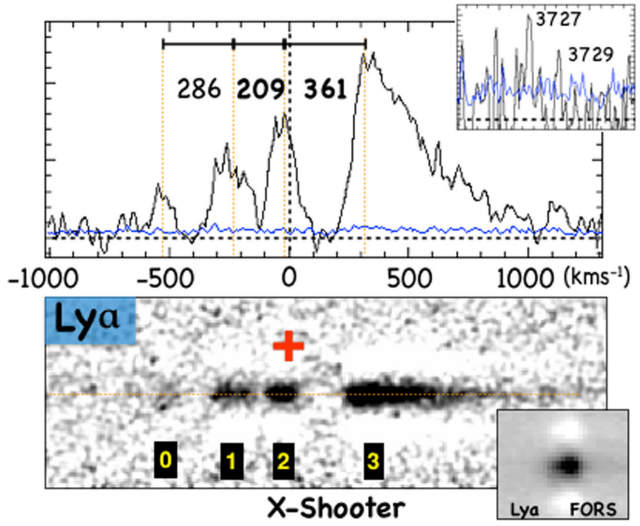

Figure 3. Top: the one-dimensional X-Shooter spectrum of the Ly α is shown (at $dv \simeq 35$ km s^{-1}) in the velocity space (with reported the relative velocities among the peaks, km s^{-1}). The systemic velocity is inferred from the [O II]λ3727, 3729 doublet (top-right inset) and marked with the red cross. Bottom: the X-Shooter two-dimensional spectrum is shown with the four main structures identified. In the bottom-right inset the same Ly α line is shown at resolution d$v \simeq 600$ km s^{-1} as observed with FORS.

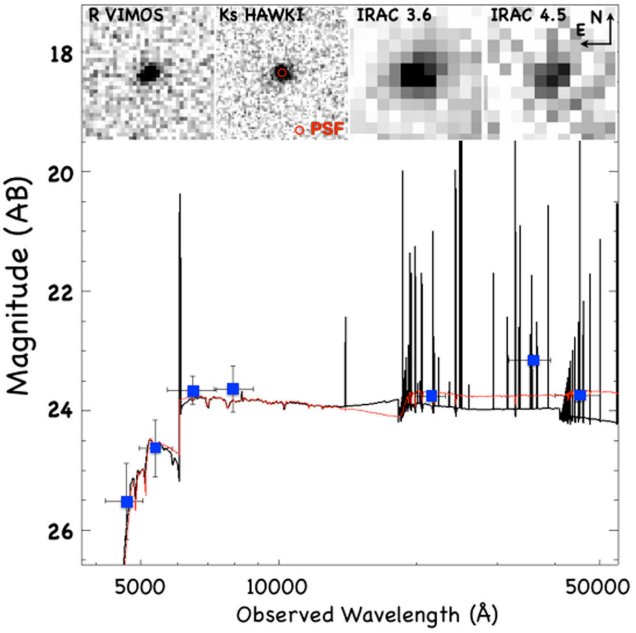

Figure 4. The cutouts of *Ion3* (top, 6.6 arcsec across) and the best SED fitted with only stellar (red) and stellar and nebular (black) templates are shown. The photometric jump at 3.6 μm is evident.

d$v \simeq -400 \pm 150$ km s^{-1}. This is also consistent with the well developed red tail of peak (3) possibly suggesting backscattering from the receding gas.

Interestingly, a very similar direct Ly α escape has recently been identified in a lensed $z = 2.37$ galaxy by Rivera-Thorsen et al. (2017), in which the central peak is also at the systemic redshift and indicative of a possible perforated channel of very low H I optical depth.

3.4 Physical properties from the SED fitting and the nature of the ionizing radiation

SED fitting has been performed using BC03 templates (Bruzual & Charlot 2003) including the nebular prescription and assuming exponentially declining star formation histories with *e*-folding time $0.1 < \tau < 15$ Gyr, (see Castellano et al. 2016 for details). It has been applied to the ground-based ESO/WFI imaging ($B_{[842]}$, $V_{[843]}$, $R_{[844]}$, and $Ic_{[879]}$, and deep ESO VLT/HAWKI K_s (obtained with 0.39 arcsec seeing, Brammer et al. 2016) and space-based Sptizer/IRAC 3.6 and 4.5 μm bands[1] (see Fig. 4). While *Ion3* is detected at S/N $\lesssim 5$ in the ESO/WFI bands, the optical rest-frame continuum is detected with S/N $\gtrsim 10$ in the Ks and IRAC bands. The most interesting features are the flat continuum at rest-frame wavelengths 4400 and 9000 Å, and the clear excess in the 3.6 μm band consistent with an H α emission with rest-frame EW of 1000Å. The best-fitting solution implies *Ion3* is a relatively low stellar mass ($1.5 \times 10^9 M_\odot$) system undergoing a starburst phase (SFR $\simeq 140$ M$_\odot$yr^{-1}) consistently with the presence of prominent Ly α, N Vλ1240 P-Cygni profile, strong H α and measured LyC. *Ion3* appears as a still rapidly growing system with a specific star formation rate of $\simeq 90$ Gyr^{-1} (see Table 1 for a summary of the properties of *Ion3*). The photometric estimate of the H α line luminosity ($\simeq 2 \times 10^{43}$ erg s^{-1}) implies a high LyC photon production efficiency, $\xi_{\rm ion} = 25.6 \pm 0.2$ (Hz erg^{-1}). It resembles the values derived by Bouwens et al. (2016) for the bluest galaxies ($\beta < -2.3$, see also Shivaei et al. 2017), and consistent with the values reported from local candidate and confirmed LyC emitters, that also show large rest-frame EW(H α) $\sim$1000 Å (e.g. Izotov et al. 2017; Jaskot et al. 2017), and eventually similar to those inferred at $z > 6$ reported by Stark et al. (2017). It is also worth noting that *Ion3* belongs to the starburst region of the $z \sim 4.5$ SFR$-$M* bimodal distribution recently identified by Caputi et al. (2017). Based on current data, there is no evidence of, nor any need for, any contribution to the UV emission by an AGN. The relatively large ratios of Ly α/ N V ($\simeq 17 \pm 2$) and Ly α/ C IV $\gtrsim 20$ tend to exclude the presence of an obscured AGN (e.g. Alexandroff et al. 2013). A relatively shallow *Chandra* exposure of 130 ksec in the 0.5–2 kev band available in the field 1 yields a limit of 1.6×10^{-15} erg s^{-1} cm^{-2} (3σ), corresponding to an upper limit to the X-ray luminosity of 3×10^{43} erg s^{-1}, which rules out a luminous AGN. Assuming a low-luminosity AGN is present, the very young burst detected would imply the ionizing photons are a mixture of stellar and non-stellar radiation escaping along a transparent medium ($N_{\rm HI} < 10^{17.2}$ cm^{-2}), that, however, should not be able to attenuate the expected high-ionization emission lines, making *Ion3* either a very special case among the AGN category or a pure star-forming dominated object. Another possibility is that *Ion3* has been captured just after the AGN has turned off, such that the optically thin channel produced by the previous nuclear activity enables the Ly α and LyC stellar radiation to escape towards the observer.

4 FINAL REMARKS

Ion3 is a bright star-forming galaxy showing copious LyC leakage identified just 1.5 Gyr after the Big-Bang ($z = 4$). This makes *Ion3* the highest redshift confirmed LyC emitter known so far. In particular,

[1] http://www.stsci.edu/hst/campaigns/frontier-fields/FF-Data

(i) The spectral features and the SED-fitting suggest that *Ion3* is a young, low-mass system undergoing a starburst phase containing hot and massive stars, with a specific star formation rate of 90 Gyr^{-1}.

(ii) The FORS and X-Shooter spectra reveal for the first time at such redshift a transparent ionized channel through which the Ly α photons escape at the resonance frequency, plausibly along the same path of the LyC photons.

The absence of HST imaging prevents us from deriving any conclusion on the morphology of the galaxy. The image with the best seeing is the VLT/HAWKI Ks-band (0.39 arcsec) from which *Ion3* appears marginally resolved with a FWHM ∼2–3 kpc proper. We refer the reader to a future work focused on the detailed analysis of the spatial distribution of the ionizing and non-ionizing radiation, as well as a proper radiative transfer modelling of the Ly α emission. However, it is worth noting that *Ion3* shows similar properties of another LyC emitter we identified at $z = 3.21$ (dubbed *Ion2*, Vanzella et al. 2016), e.g. a structured Ly α shape, the blue UV slope and weak low-ionization interstellar absorption lines. While in the case of *Ion2* we confirmed also very strong [O III]λ5007 lines (EW > 1000 Å rest-frame) and large O32 index ([O III]λ5007/[O II]λ3727 > 10) making it among of the highest redshift Green Pea galaxy and suggesting a density-bounded condition, *Ion3* might also have a perforated medium and will need JWST to probe the rest-frame optical wavelengths (imaging and spectroscopy) and HST to image directly the LyC. Irrespective of the nature of the ionizing radiation, *Ion3* represents a unique high-redshift laboratory where ionized channels carved in the interstellar medium by one or more feedback sources can be studied. *Ion3* and *Ion2* represent ideal reference cases to guide the search for reionizing sources at $z > 6.5$ with JWST.

ACKNOWLEDGEMENTS

We thank the referee for constructive comments. EV gratefully acknowledge the excellent support by ESO staff at Paranal during the observations. We thank G. Zamorani, A. Jaskot, S. Oey, D. Schaerer and A. Grazian for useful discussions. FC, AM acknowledge funding from the INAF PRIN-SKA 2017 program 1.05.01.88.04. MM acknowledges support from the Italian Ministry of Foreign Affairs and International Cooperation, Directorate General for Country Promotion. Based on observations collected at the European Southern Observatory for Astronomical research in the Southern hemisphere under ESO programmes P098.A-0804(B), P098.A-0665(B).

REFERENCES

Alexandroff R. et al., 2013, MNRAS, 435, 3306
Behrens C., Dijkstra M., Niemeyer J. C., 2014, A&A, 563, 77
Bian F., Fan X., McGreer I., Cai Z., Jiang L., 2017, ApJ, 837, L12
Bouwens R., Smit R., Labbé I., Franx M., Caruana J., Oesch P., Stefanon M., Rasappu N., 2016, ApJ, 831, 176
Brammer G. B. et al., 2016, ApJS, 226, 6
Bruzual G., Charlot S., 2003, MNRAS, 344, 1000
Caminha G. B. et al., 2016, A&A, 587, 80
Caputi K. I. et al., 2017, ApJ, 849, 45
Castellano M. et al., 2016b, A&A, 590, A31
Chisholm J., Orlitová I., Schaerer D., Verhamme A., Worseck G., Izotov Y. I., Thuan T. X., Guseva N. G., 2017, A&A, 605, 67
de Barros S. et al., 2016, A&A, 585, A51
Grazian A. et al., 2017, A&A, 602, A18
Heckman T. M. et al., 2011, ApJ, 730, 5
Henry A., Scarlata C., Martin C. L., Erb D., 2015, ApJ, 809, 19
Inoue A. K., Shimizu I., Iwata I., Tanaka M., 2014, MNRAS, 442, 1805
Izotov Y. I., Schaerer D., Thuan T. X., Worseck G., Guseva N. G., Orlitová I., Verhamme A., 2016a, MNRAS, 461, 3683
Izotov Y. I., Orlitová I., Schaerer D., Thuan T. X., Verhamme A., Guseva N. G., Worseck G., 2016b, Nature, 529, 178
Izotov Y. I., Schaerer D., Worseck G., Guseva N. G., Thuan T. X., Verhamme A., Orlitova I., Fricke K. J., 2017, MNRAS, 474, 4514
Jaskot A. E., Oey M. S., 2013, ApJ, 766, 91
Jaskot A. E., Oey M. S., 2014, ApJ, 791, L19
Jaskot A. E., Oey M. S., Scarlata C., Dowd T., 2017, ApJ, 851, L6
Jones T. A., Ellis R. S., Schenker M. A., Stark D. P., 2013, ApJ, 779, 52
Leitherer C., Ekström S., Meynet G., Schaerer D., Agienko K. B., Levesque E. M., 2014, ApJS, 212, 14
Lotz J. M. et al., 2017, ApJ, 837, 97
Nakajima K., Ouchi M., 2014, MNRAS, 442, 900
Rivera-Thorsen T. E. et al., 2017, A&A, 608, 4
Salpeter E. E., 1955, ApJ, 121, 161
Schaerer D., Izotov Y. I., Verhamme A., Orlitová I., Thuan T. X., Worseck G., Guseva N. G., 2016, A&A, 591, 8
Shapley A., Steidel C. C., Strom A. L., Bogosavljevic M., Reddy N. A., Siana B., Mostardi R. E., Rudie G. C., 2016, ApJ, 826, 24
Shivaei I. et al., 2017, preprint (arXiv:1711.00013)
Siana B. et al., 2015, ApJ, 804, 17
Stark D. P. et al., 2017, MNRAS, 464, 469
Vanzella E., Siana B., Cristiani S., Nonino M., 2010, MNRAS, 404, 1672
Vanzella E. et al., 2012, ApJ, 751, 70
Vanzella E. et al., 2014, ApJ, 783, L12
Vanzella E. et al., 2015, A&A, 576, A116
Vanzella E. et al., 2016, ApJ, 825, 41
Vanzella E. et al., 2017, ApJ, 842, 47
Verhamme A., Orlitová I., Schaerer D., Hayes M., 2015, A&A, 578, A7
Verhamme A., Orlitová I., Schaerer D., Izotov Y., Worseck G., Thuan T. X., Guseva N., 2017, A&A, 597, 13
Worseck G. et al., 2014, MNRAS, 445, 1745
Yang H., Malhotra S., Gronke M., Rhoads J. E., Dijkstra M., Jaskot A., Zheng Z., Wang J., 2016, ApJ, 820, 130
Zackrisson E., Inoue A. K., Jensen H., 2013, ApJ, 777, 39

This paper has been typeset from a TEX/LATEX file prepared by the author.